

A two zone model for the broad Iron line emission in MCG-6-30-15

R. Misra

Inter-University Centre for Astronomy and Astrophysics, Pune, India

ABSTRACT

We reanalyze the ASCA and BeppoSAX data of MCG-6-30-15, using a double zone model for the Iron line profile. In this model, the X-ray source is located around ≈ 10 Schwarzschild radius and the regions interior and exterior to the X-ray source produce the line emission. We find that this model fits the data with similar reduced χ^2 as the standard single zone model. The best fit inclination angle of the source ($i \approx 10^\circ$) for the medium intensity ASCA data set is compatible with that determined by earlier modeling of optical lines. The observed variability of the line profile with intensity can be explained as variations of the X-ray source size. That several AGN with broad lines have the peak centroid near 6.4 keV can be explained within the framework of this model under certain conditions.

We also show that the simultaneous broad band observations of this source by BeppoSAX rules out the Comptonization model which was an alternative to the standard inner disk one. We thereby strengthen the case that the line broadening occurs due to the strong gravitational influence of a Black Hole.

Subject headings: accretion disks—black hole physics—galaxies:individual (MCG-6-30-15)—galaxies:Seyfert—line:profile

1. Introduction

A long duration (4.2 days), observation of the Seyfert 1 AGN, MCG-6-30-15, revealed for the first time that the Iron line profile in this source is broad (Tanaka et al. 1995). Subsequently broad Iron lines were also detected in other AGN by ASCA (Nandra et al. 1997). Independent reconfirmation of this result came from the broad band observations of this source by BeppoSAX (Guainazzi et al. 1999). Recently a second long observation of MCG-6-30-15 by ASCA confirmed the results obtained earlier (Iwasawa et al. 1999).

Tanaka et al. (1995) pointed out that the large width of the line could probably be due to the extreme gravitational effects near the vicinity of a Black hole (Fabian et al. 1989). In this model, the emission arises from the innermost region ($\approx 6 - 10r_g$ where $r_g = GM/c^2$) of a cold accretion disk around a Black hole which is illuminated by an X-ray source. Fabian et al. (1995) considered several mechanisms for line broadening and concluded that none of them were satisfactory except the inner disk emission model. One of the alternate models considered by them is the Comptonization model first proposed by Czerny, Zbyszewska and Raine (1991). In the Comptonization model, line broadening occurs because of Compton down scattering of the emission line photons as they pass through an optically thick cloud. Misra & Kembhavi (1999) showed that a compact highly ionized cloud was not ruled out by the data available then. Subsequently, Misra & Sutaria (1999) fitted the ASCA data to the Comptonization model and found that the fit was as good as the disk emission model. However, It was pointed out by Misra & Kembhavi (1999) that simultaneous broad band data would be able to rule out or confirm the presence of such a cloud. The recent BeppoSAX broad band (0.1-200 keV) observations of this source gives such an opportunity. In this paper, we show that analysis of the BeppoSAX data indeed rules out the Comptonization model, thereby strengthening the case for the disk line model.

Despite the success of the inner disk model, the actual geometry of the source especially the position of the illuminating X-ray source is still unknown. The inner disk emission models (Fabian et al. 1989; Laor 1991) used for fitting the data, assumes a cold accretion disk inclined at a angle (i) with a power-law type radial emissivity function ($I \propto R^{-\alpha}$). Here α is called the emissivity index. Other parameters are the inner (R_i) and outer (R_o) disk radius. Spectral fitting of the ASCA data reveals that α is positive (Iwasawa 1996) which implies that the X-ray source must be located near or at a radius less than the inner edge of the disk ($6 - 1.2r_g$). This is contrary to standard models for the X-ray production in which the source is located where the maximum gravitational energy is dissipated ($\approx 10r_g$). In particular, the hot disk model, in which the X-rays are generated in an inner hot region of disk (Shapiro, Lightman & Eardley 1976) is ruled out. The X-ray source may then be in the form of a hot corona on top of the cold disk (Liang & Price 1977). Even, here the Iron line modeling restricts the location of the corona to be only over the inner edge of the disk and not around $10r_g$. It is important to study the constrains imposed by the Iron line profile fitting in detail, since it may significantly change the standard X-ray production models or force introduction of relatively new ones (for e.g. the X-ray source located in the form of a jet).

The disk line fit to MCG-6-30-15 to the ASCA data constrains the inclination angle $i \approx 30^\circ$ (Iwasawa et al. 1996). This is contrary to the inclination angle derived by modeling

the optical $H\alpha$ measurements for the same source (Sulentic et al. 1998). Recently Rokaki & Boisson (1999) developed an accretion disk model for both the UV continuum and the optical lines from AGN. They also found that for MCG-6-30-15, the best fit inclination angle $i \approx 12^\circ$. This discrepancy could be due to a) the optical line are not produced in the outer regions of the accretion disk, b) the disk is warped or c) that the disk line model is simplistic i.e. the geometry assumed is not a good approximation. That the geometry of the disk line model is complex is also indicated by the study of several AGN with broad line which revealed that many of them have their peak centroid close to 6.4 keV. It was pointed out by Sulentic, Marziani & Calvani (1998) that this is not expected if the disks are oriented in random directions. Taking these arguments into account Sulentic, Marziani & Calvani (1998) suggested that perhaps the line profile is a sum of two independent components. Alternatively, Blackman (1999) suggested that this could be due to a concave inner accretion disk.

In this paper, we reanalyze the ASCA and BeppoSAX observation of MCG-6-30-15 to study whether the Iron line profile could really be a sum of two components and whether the line profile modeling can be made more compatible with the standard X-ray production models. In particular, if the X-ray source is located near $\approx 10r_g$, there will be two distinct regions for line production. One will be the inner most region with radii less than the X-ray producing source. Here the emissivity index (α) would be negative. There would also be a second region with radii greater than the X-ray source where α would be positive. We allow for the possibility that near the X-ray source, line emission may not arise due to the absence of cold accretion disk or if the disk is highly ionized.

2. Results

ASCA observed MCG-6-30-15 for ≈ 4.2 days from 1994 July 23 to 27 (Tanaka, Inoue & Holt 1994). This long exposure allowed for the first time the detection of a broad Iron line (Tanaka et al. 1995). A subsequent detailed analysis by Iwasawa et al. (1996) showed that the line shape was variable and correlated to the intensity of the source. Iwasawa et al. (1996) grouped the data into three intensity levels called the low (LI), medium (MI) and high intensity (HI) data sets. During most (3/4) of the observation time, the source was in the medium intensity level. Iwasawa et al. fitted the line profile with a phenomenological two Gaussian model and accretion disk models around stationary (Schwarzschild) and rotating (Kerr) Black holes. This data has also been reanalyzed using alternate models like a Comptonizing cloud model (Misra & Sutaria 1999) and an occultation model (Weaver & Yaqoob 1998).

Following Iwasawa et al. (1996) we divide the data into the three different intensity levels. We analyze the 3 – 10 keV data since below 3 keV the spectrum is affected by the partially ionized gas (“the warm absorber”) surrounding the source. Data from both the SIS chips (SIS 1 and 2) for the Bright and Bright2 modes were grouped and analyzed together. Only the relative normalization between these four sets of data was allowed to vary, but in all cases the variation was found to be less than 2%.

In table 1, we summarize the results for fitting the medium intensity (MI) data set. We start with fitting the data with the standard single zone accretion disk model (xspec model “diskline” , Fabian et al. 1989), which through out this paper we refer to as the standard disk model. To be consistent with the broad band BeppoSAX results (Guainazzi et al. 1999) we include the possibility of an Iron edge in the spectrum with threshold energy fixed at 7.6 keV. The inner edge of the accretion disk is fixed at $6 r_g$. We also fit the data with a nearly maximally rotating Black hole model (xspec model “laor” , Laor 1991) with the inner edge fixed at $1.2 r_g$. Both the models fit the data equally well with $\Delta\chi^2 = 2$ for 1421 degrees of freedom between them. These results are consistent with those reported by Iwasawa et al (1996). An additional Gaussian line emission is not required for this model. The angle of inclination (i) is well constrained for both the fits to be $\approx 30^\circ$. So fixing the inclination angle to be 10° gives a unacceptable increase in $\Delta\chi^2 = 82$ (Table 1: row 3). However, an addition of a narrow Gaussian line with centroid energy of 6.4 keV reduces χ^2 by 52 (Table 1: column 4). Thus if the inclination angle for the source is restricted to be around 10° by some other observational constrain (e.g. modeling of the optical lines by Sulentic et al. 1998), then an additional component will be required to explain the ASCA observations considered here. If i is fixed at 20° a similar result is obtained (reduced $\chi^2 = 1420$ for 1421 degrees of freedom), however the strength and significance of the narrow Gaussian line is slightly reduced ($I_g = 3 \times 10^{-5}$ photons $\text{sec}^{-1} \text{cm}^{-3}$). The reduced χ^2 for the model with a constrained inclination angle is still significantly higher than the standard disk model (Table 1: column 1).

An additional component in the line shape, if present, would also be expected to arise from close to the Black hole, since this feature is also variable in short time scales ($< \text{hrs}$). There could be two regions in the inner accretion disk which produces the Iron line. Such a double zone region is expected if the X-ray source is located near the radius of maximum gravitational energy dissipation ($\approx 10r_g$). The picture would then be of a cold accretion disk with an X-ray source in the form of an extended corona around $10r_g$. Alternately, the X-ray producing region could be a hot accretion disk around $10r_g$ with a cold outer disk and an inner region which is again cold. In either case there would be an inner most line emitting region ($6r_g < R < 10r_g$) where the emissivity index (α where $I \propto R^{-\alpha}$) would typically be positive. A outer second region ($10r_g < R$) would also be impinged by the

Table 1: Spectral Parameters for the ASCA medium intensity data set. Parameters without errors were fixed during fitting.

Model param.	Units					
E_{th}	keV	7.6	7.6	7.6	7.6	7.6
τ		$0.09^{+0.06}_{-0.06}$	$0.04^{+0.09}_{-0.04}$	$0.22^{+0.06}_{-0.06}$	$0.14^{+0.06}_{-0.06}$	$0.11^{+0.06}_{-0.06}$
N_H	10^{20} cm^{-2}	6.4	6.4	6.4	6.4	6.4
Γ		$2.01^{+0.03}_{-0.03}$	$2.04^{+0.05}_{-0.05}$	$1.91^{+0.02}_{-0.03}$	$1.97^{+0.03}_{-0.03}$	$2.00^{+0.03}_{-0.03}$
i	deg	$31.7^{+1.0}_{-1.0}$	$32.1^{+1.8}_{-1.6}$	10	10	$11.4^{+1.4}_{-1.2}$
E_{d1}	keV	6.4	6.4	6.4	6.4	6.7
α_1		$1.25^{+0.75}_{-0.83}$	$1.60^{+0.6}_{-0.7}$	$2.86^{+0.19}_{-0.14}$	$3.46^{+0.35}_{-0.31}$	-3.0
R_{i1}	r_g	6.0	1.2	6.0	6.0	6.0
R_{o1}	r_g	17^{+2}_{-1}	$17.6^{+3.8}_{-1.9}$	1000	33^{+15}_{-8}	$8.6^{+0.5}_{-0.8}$
I_{d1}	$10^{-5} \text{ s}^{-1} \text{ cm}^{-2}$	$15.9^{+1.2}_{-1.4}$	$20.0^{+4.0}_{-3.5}$	$8.2^{+1.0}_{-1.1}$	$8.6^{+1.1}_{-1.0}$	$6.5^{+0.8}_{-0.9}$
E_{d2}	keV	-	-	-	-	6.7
α_2		-	-	-	-	3.0
R_{i2}	r_g	-	-	-	-	$12.7^{+1.5}_{-1.3}$
R_{o2}	r_g	-	-	-	-	1000
I_{d2}	$10^{-5} \text{ s}^{-1} \text{ cm}^{-2}$	-	-	-	-	$7.8^{+0.9}_{-0.8}$
I_g	$10^{-5} \text{ s}^{-1} \text{ cm}^{-2}$	-	-	-	$3.9^{+0.5}_{-0.6}$	-
$\chi^2/(\text{dof})$		1381(1421)	1379 (1421)	1463(1422)	1411(1421)	1380 (1420)

X-rays but in this case α would be expected to be negative. The two regions will be distinct if the X-ray source is an hot disk in between the two. On the other hand, if the X-ray source is in the form of a corona, the underlying cold disk may be highly ionized and line emission may not arise from around $10r_g$. We approximate the complex geometry above by a simple model consisting of two standard disk line models (i.e. two xspec model: “diskline”). For the first diskline model the inner radius (R_{i1}) is held constant at $6r_g$ and the emissivity index (α_1) is fixed at a constant negative value ($= -3$). The outer radius (R_{o1}) is a free parameter. For the second diskline model the outer radius (R_{o2}) is held constant at a large value ($= 1000r_g$), while the inner radius (R_{i2}) is a free parameter. The emissivity index (α_2) is fixed at a constant positive value ($= 3$). The results obtained here are not very sensitive to the actual values of (α) chosen if α_1 is taken to be negative and α_2 is taken to be positive. In this phenomenological description, the region of the disk between ($R_{o1} < r < R_{i2}$) is either the X-ray producing hot disk or where the cold disk is highly ionized. This model will be referred to in this paper as the double zone model. Table 1: column 5 shows the result of fitting such a model to the ASCA MI data set. The reduced χ^2 is similar to the one obtained using the standard disk model. The best fit inclination angle ($i \approx 10^\circ$) agrees well with the value obtained on modeling the optical line emission from the source (Sulentic et al. 1988). A better fit to the spectrum is obtained if the rest frame energy of the line emission from both the regions is 6.7 keV. This indicates that the Iron in the cold disk is partially ionized. The line profile for the double zone model is shown in figure 1. We note that the combined line profile can be complex with several features. In simple disk line fits, these features may be interpreted as an absorption edge around ≈ 6 keV as was done for another AGN, NGC 3516 by Nandra et al. (1999).

Table 2 summarizes the results obtained by fitting the above models to the ASCA high intensity (HI) data set. Since the statistics for this data set is lower than for the MI data set, some parameters (τ , i , α and R_{o1}) have been fixed. As pointed out by Iwasawa et. al. (1996) the HI data set is not well described by the standard disk line model and an additional narrow line Gaussian is required (reduced χ^2 decreases by 20). The double zone model also fits the data better than the standard disk line one (reduced χ^2 decreases by 14).

Table 3 summarizes the results obtained by fitting the above models to the ASCA low intensity (LI) data set. In this intensity level the source exhibits an extended red wing which has been interpreted as emission from a disk that extends to less than $6r_g$ which would imply that the Black hole is spinning at a nearly maximal rate (Iwasawa et al. 1996). Here also we find that the $\Delta\chi^2 = 4$ (for 153 dof) between the two models (Table 3: column 1 and 2). However, as pointed out by Weaver & Yaqoob (1998) although this difference is statistically significant the inclusion of systematic errors may decrease its overall significance. Moreover, the spectral calculations of this models are approximate and

Table 2: Spectral Parameters for the ASCA high intensity data set. Parameters without errors were fixed during fitting.

Model parameters	Units				
E_{th}	keV	7.6	7.6	7.6	7.6
τ		0.1	0.1	0.1	0.1
N_H	10^{20} cm^{-2}	6.4	6.4	6.4	6.4
Γ		$1.96^{+0.07}_{-0.03}$	$1.98^{+0.08}_{-0.08}$	$1.92^{+0.08}_{-0.03}$	$1.98^{+0.04}_{-0.05}$
i	deg	30	30	10	10
E_{d1}	keV	6.4	6.4	6.4	6.7
α_1		2.0	2.0	3.5	-3.0
R_{i1}	r_g	6.0	1.23	6.0	6.0
R_{o1}	r_g	$28.5^{+16}_{-10.2}$	$15.1^{+0.9}_{-0.9}$	35	8.5
I_{d1}	$10^{-5} \text{ ph s}^{-1} \text{ cm}^{-2}$	$11.8^{+5.4}_{-3.0}$	$12.1^{+4.7}_{-2.5}$	$1.7^{+3.4}_{-1.7}$	$4.0^{+2.3}_{-2.0}$
E_{d2}	keV	-	-	-	6.7
α_2		-	-	-	3.0
R_{i2}	r_g	-	-	-	$17.5^{+5.0}_{-3.5}$
R_{o2}	r_g	-	-	-	1000
I_{d2}	$10^{-5} \text{ ph s}^{-1} \text{ cm}^{-2}$	-	-	-	$8.6^{+1.4}_{-1.4}$
I_g	$10^{-5} \text{ ph s}^{-1} \text{ cm}^{-2}$	-	-	$6.3^{+1.5}_{-1.5}$	-
$\chi^2/(\text{dof})$		506(497)	500(497)	486(496)	491(496)

for simple geometries. It should be noted that for $R = 6r_g$ and inclination angle $i = 0^\circ$, the red-shift, $E_{obs}/E_{emit} = (1 - 3r_g/r)^{1/2} = 0.707$ which means $E_{obs} = 4.5$ keV for 6.4 keV rest frame photons (Hanawa 1989). A similar exercise for $i = 90^\circ$, shows that the maximum $E_{obs} = 9$ KeV and the minimum $E_{obs} = 3$ keV. Hence just the detection of photons at 4 keV does not necessarily imply that the metric is Kerr. The spectral fit for Kerr is better than the Schwarzschild case because of the difference in spectral shape. For the double zone model, if both R_{i2} and R_{o1} are allowed to be free parameters then the unphysical result of $R_{o1} > R_{i2}$ is obtained. Hence, for this data set we have imposed the condition $R_{o1} = R_{i2}$. The reduced χ^2 obtained is similar to the standard disk model (columns 1 and 4). If the rest frame energy of the inner region is 6.4 keV the reduced χ^2 obtained is similar to the rotating Black hole case (columns 2 and 5). Since the X-ray luminosity is lower in this data set, the inner disk may indeed be at a lower ionized state. The line profile for the double zone model is shown in figure 2.

MCG-630-15 was observed by BeppoSAX from 1996 July 29 to August 3 using the Low Energy Concentrator Spectrometer (LECS, 0.1 – 4 keV), the Medium Energy Concentrator Spectrometer (MECS, 1.8 – 10.5 keV) and the Phoswich Detector System (PDS, 17 – 200 keV) (Guainazzi et al. 1999). The low energy spectrum is affected by the presence of “a warm absorber”. Following Guainazzi et al. (1999) and Orr et al. (1997) we parameterized the warm absorber as absorption edges with threshold energies: 0.74 keV (O VII), 0.87 keV (O VIII) and 1.2 keV (Ne IX) and the following emission lines with centroid energies: 0.62 keV (K_α O VII) and 0.86 keV (iron-L). We also added an absorption edge with threshold energy 7.6 keV which corresponds approximately to Fe XV absorption. For the continuum, an exponentially cutoff power-law with a Compton reflection component (Xspec model: “pexrav”, Magdziarz & Zdziarski 1995) was used.

Table 4 summarizes the result of fitting the various Iron line models to the BeppoSAX data set. As reported by Guainazzi et al. (1999) the standard disk model fits the data well. Like the ASCA results the inclination angle is well constrained to be $i \approx 35^\circ$ and constraining $i = 10^\circ$ requires an additional Gaussian line (Table 4: column 2 and 3). The double zone model also fits the data well but the inner line producing region is somewhat smaller than the ASCA results ($R_{o1} \approx 6.2r_g$).

An alternate model to the disk line emission model is the Comptonization model where the line is broadened due Compton down scattering of the photons as they pass through an optically thick cloud. Misra & Sutaria (1999) showed that this model fits the narrow band ASCA data for this source. They had also pointed out that the broad band simultaneous data obtained by BeppoSAX may rule out or confirm the model. Fitting this model to the BeppoSAX data we obtain a reduced $\chi^2 = 136$ for 121 degrees of freedom. Since this

Table 3: Spectral Parameters for the ASCA low intensity data set. Parameters without errors were fixed during fitting.

Model parameters	Units					
E_{th}	keV	7.6	7.6	7.6	7.6	7.6
τ		0.1	0.1	0.1	0.1	0.1
N_H	10^{20} cm^{-2}	6.4	6.4	6.4	6.4	6.4
Γ		$1.78^{+0.14}_{-0.11}$	$1.81^{+0.15}_{-0.12}$	$1.77^{+0.12}_{-0.12}$	$1.78^{+0.14}_{-0.11}$	$1.81^{+0.12}_{-0.12}$
i	deg	30	30	10	10	10
E_{d1}	keV	6.4	6.4	6.4	6.7	6.4
α_1		$1.1^{+0.5}_{-5.3}$	$2.1^{+0.7}_{-1.2}$	3.5	-3.0	-3.0
R_{i1}	r_g	6.0	1.23	6.0	6.0	6.0
R_{o1}	r_g	15.5	15.5	35	$7.8^{+0.6}_{-0.6}$	$9.1^{+0.6}_{-0.6}$
I_{d1}	$10^{-5} \text{ ph s}^{-1} \text{ cm}^{-2}$	$15.5^{+4.7}_{-5.0}$	$21.4^{+7.5}_{-6.3}$	$10.4^{+3.0}_{-2.4}$	$5.5^{+2.1}_{-3.7}$	$6.7^{+1.9}_{-2.2}$
E_{d2}	keV	-	-	-	6.7	6.7
α_2		-	-	-	3.0	3.0
R_{i2}	r_g	-	-	-	7.8	9.1
R_{o2}	r_g	-	-	-	1000	1000
I_{d2}	$10^{-5} \text{ ph s}^{-1} \text{ cm}^{-2}$	-	-	-	$9.0^{+5.6}_{-2.6}$	$9.1^{+5.3}_{-2.1}$
I_g	$10^{-5} \text{ ph s}^{-1} \text{ cm}^{-2}$	-	-	$3.4^{+1.5}_{-1.4}$	-	-
$\chi^2/(\text{dof})$		172(153)	168 (153)	172(153)	171(152)	168(152)

Table 4: Spectral Parameters for the BeppoSAX data set. Parameters without errors were fixed during fitting.

Model parameters	Units				
E_{th}	keV	7.6	7.6	7.6	7.6
τ		$0.14^{+0.03}_{-0.04}$	$0.19^{+0.04}_{-0.03}$	$0.17^{+0.03}_{-0.05}$	$0.16^{+0.03}_{-0.04}$
N_H	10^{20} cm^{-2}	$6.4^{+0.2}_{-0.3}$	$6.1^{+0.2}_{-0.3}$	$6.3^{+0.2}_{-0.3}$	$6.2^{+0.3}_{-0.2}$
Γ		$1.99^{+0.03}_{-0.04}$	$1.94^{+0.03}_{-0.04}$	$1.96^{+0.04}_{-0.04}$	$1.97^{+0.04}_{-0.04}$
E_{cut}	keV	108^{+57}_{-39}	82^{+31}_{-20}	91^{+40}_{-23}	101^{+49}_{-27}
R_{refl}		$0.77^{+0.23}_{-0.21}$	$0.67^{+0.23}_{-0.20}$	$0.72^{+0.22}_{-0.21}$	$0.65^{+0.22}_{-0.18}$
i	deg	37^{+2}_{-2}	10	10	10
E_{d1}	keV	6.4	6.4	6.4	6.7
α_1		2.0	$1.4^{+1.1}_{-3.0}$	3.5	-3.0
R_{i1}	r_g	6.0	6.0	6.0	6.0
R_{o1}	r_g	$7.5^{+2.4}_{-1.0}$	1000	$8.0^{+6.8}_{-1.5}$	$6.2^{+1.2}_{-0.2}$
I_{d1}	$10^{-5} \text{ ph s}^{-1} \text{ cm}^{-2}$	$9.5^{+1.7}_{-2.0}$	$3.0^{+1.3}_{-0.9}$	$2.6^{+1.3}_{-1.2}$	$2.8^{+3.4}_{-1.1}$
E_{d2}	keV	-	-	-	6.7
α_2		-	-	-	3.0
R_{i2}	r_g	-	-	-	13^{+5}_{-4}
R_{o2}	r_g	-	-	-	1000
I_{d2}	$10^{-5} \text{ ph s}^{-1} \text{ cm}^{-2}$	-	-	-	$4.4^{+1.2}_{-0.9}$
I_g	$10^{-5} \text{ ph s}^{-1} \text{ cm}^{-2}$	-	-	3.5	-
$\chi^2/(\text{dof})$		120(123)	132(123)	123(123)	124 (123)

is significantly worse than the standard disk model, the Comptonization model can be formally rejected thereby confirming that the line broadening is due to gravitational effects.

3. Summary and Discussion

In this paper, we show that a double zone model for the broad Iron line in AGN fits the ASCA and BeppoSAX data for MCG-6-30-15. In this model, the X-ray source is located around $\approx 10r_g$ of the accretion disk where there is maximum gravitational energy dissipation. The line emission arises from an innermost disk region ($\approx 7r_g$) and from a region outside the X-ray source (i.e. with radii $\approx 15r_g$). The ASCA data reveals that for this model the inclination angle of the source $i \approx 10^\circ$ which is compatible with that obtained by modeling of optical line emission from the same source (Sulentic et al. 1998).

For several AGN the centroid of the blue wing is ≈ 6.4 keV even though the width of the line varies among the sources (Nandra et al. 1997; Sulentic, Marziani & Calvani 1998). The double zone model may be able to explain these observations, if for most AGN the outer zone has a larger inner radius (i.e. R_{i2} is generally larger than what is obtained for MCG-6-30-15) and the outer region is not highly ionized i.e. the rest frame energy of the line photon is 6.4 keV. Note that in the two zone model the width of the combined line depends on the flux from the inner region. Hence the blue and the red parts of the profile may vary independently of each other. However, this speculation can only be confirmed after detailed spectral fits by the double zone model for several AGN is undertaken.

In the framework of the double zone model, the variability of MCG-6-20-15 can be explained by variation in R_{i2} , R_{o1} and/or the ionization state of the cold disk. Variations of R_{i2} and R_{o1} reflect the changing size of the X-ray emitting region with intensity. However, the data is not statistically good enough to give any concrete trends.

Although the spectral shapes for the Iron line from the standard disk model and the double zone one are similar it may be possible to differentiate them by high resolution future spectroscopy by satellites like XMM. One may also be able to rule out or confirm this model by obtaining more concrete and independent estimation of the inclination angle of MCG-6-30-15.

The author would like to thank Max Calvani and Mateo Guainazzi for useful discussions and for making available the BeppoSAX data. The author would also like to thank F. Sutarina for help with the X-ray data analysis. This research has made use of data obtained from the High Energy Astrophysics Science Archive Research Center (HEASARC), provided

by NASA's Goddard Space Flight Center.

REFERENCES

- Blackman, E.G., 1999, MNRAS, **306**, L25.
- Czerny B., Zbyszewska M. & Raine, D.J. 1991, in Treves A., ed., Iron line Diagnostics in X-ray Sources, Springer-Verlag, Berlin, p 226.
- Fabian, A.C., Rees, M.J., Stella, L. & White, N.E. 1989, MNRAS, **238**, 729.
- Fabian, A.C. et al. 1995, MNRAS, **277**, L11.
- Guainazzi M., et al., 1999, *Astron. & Astrop.*, **341**, L27.
- Hanawa, T., 1989, ApJ, **341**, 948.
- Iwasawa, K. et al. 1996, MNRAS, **282**, 1038.
- Iwasawa, K. et al. 1999, MNRAS, **306**, L19.
- Laor, A., 1991, ApJ, **376**, 90.
- Liang, E.P. & Price, R.H., 1977, ApJ, **218**, 247.
- Magdziarz, P. & Zdziarski, A. A., 1995, MNRAS, **273**, 837.
- Misra, R. & Kembhavi, A.K., 1998, ApJ, **499**, 205.
- Misra, R. & Sutaria, F. K. 1999, ApJ, **517**, 661.
- Orr A., et al. 1997, *Astron. & Astrop.*, **324**, L77.
- Nandra, K., George, I.M., Mushotzsky, R.F., Turner, T.J. & Yaqoob, T. 1997, ApJ, **477**, 602.
- Nandra, K., George, I.M., Mushotzsky, R.F., Turner, T.J. & Yaqoob, T. 1999, ApJ, *in press* (astro-ph/9907193).
- Rokaki, E. & Boisson, C., 1999, MNRAS, **307**, 41.
- Shapiro, S.L., Lightman A.P. & Eardley, D.M. 1976, ApJ, **204**, 187.
- Sulentic, J. et al., 1998, ApJ, **501** 54.
- Sulentiç, J., Marziani, P. & Calvani, M., 1998, ApJ, **497**, L65
- Tanaka, Y., Inoue, H. & Holt, S.S., 1994, PASJ, **46**, L137
- Tanaka, Y. et al., 1995, Nature, **375**, 659.

Weaver, K. A. & Yaqoob, T., 1998, ApJ, **502**, L139.

Fig. 1.— The line profile for the ASCA medium intensity (MI) data set. The dashed lines are the profiles from the inner and outer regions. The parameters for the fit are from Table 1: column 5

Fig. 2.— The line profile for the ASCA low intensity (LI) data set. The dashed lines are the profiles from the inner and outer regions. The parameters for the fit are from Table 3: column 5

Figure 1

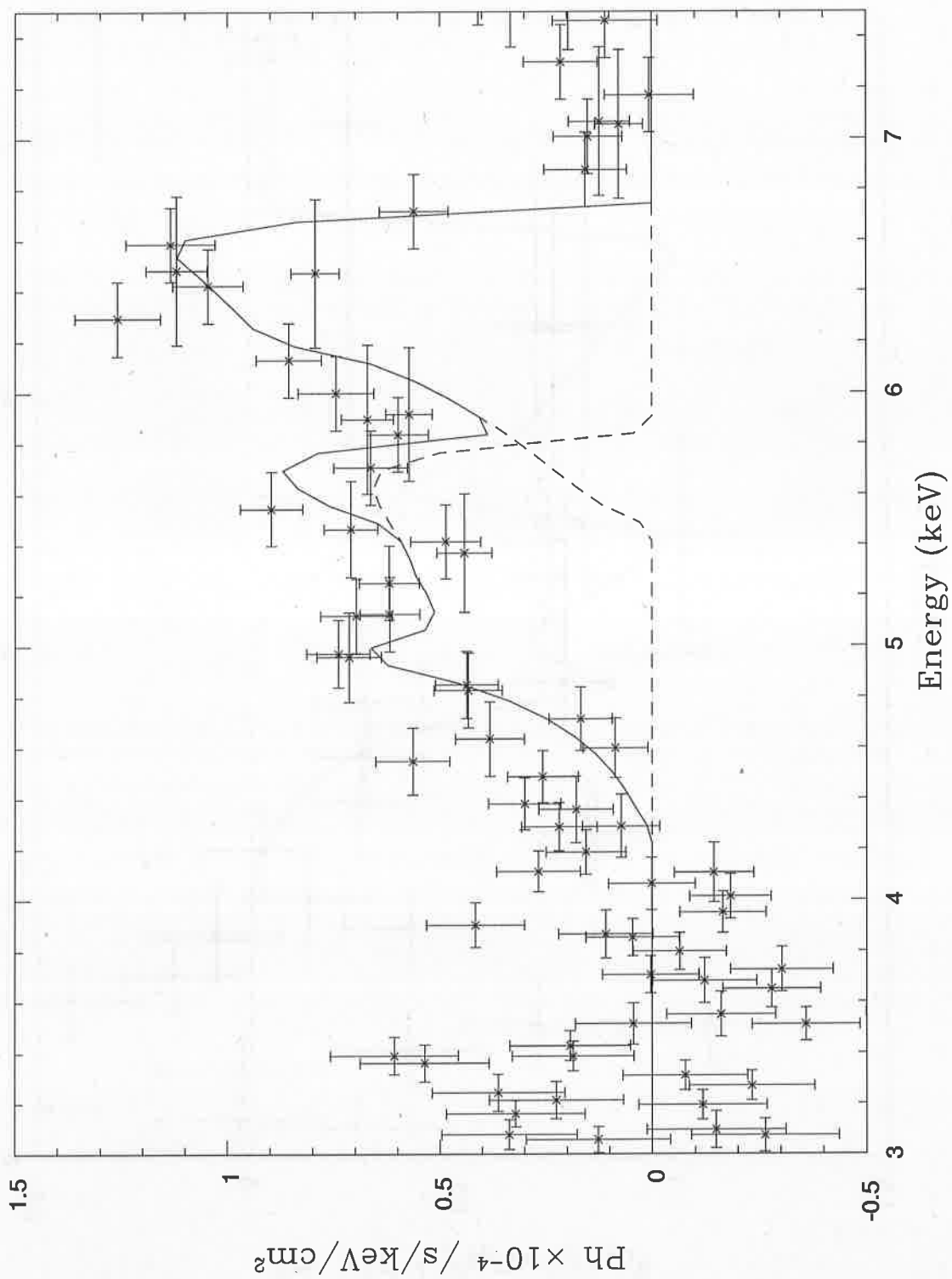


Figure 2

